Excitation of the He $1\,^1S-2\,^3S$ transition by electrons and photons: A QED approach

Sujata Bhattacharyya* and Sanchita Mitra
Gokhale Memorial Girls' College, Calcutta 700 020, India
(Received 19 November 1998)

A field-theoretic study of the simultaneous electron-photon excitation (SEPE) and direct electron excitation (DEE) is done for the He $1\,^1S\rightarrow 2\,^3S$ transition by spin polarized electrons in the field of soft photons. The ratio of SEPE to DEE is found to lie around 3×10^{-3} for the 0.117-eV photon and incident electron of energy E_i between 19.817 and 20 eV. The present result is compared with the existing experimental data. [S1050-2947(99)00409-6]

PACS number(s): 34.80.Dp, 82.30.Fi

I. INTRODUCTION

A field-theoretic study of the simultaneous electron-photon excitation (SEPE) and direct electron excitation (DEE) of He by electrons in the transition from $1\,^1S-2\,^3S$ is reported respectively for the reactions

$$\mathrm{He}(1s^2\,^1S)+e^-(E_i)+h\nu\rightarrow\mathrm{He}(1s2s\ ^3S)+e^-(E_f=E_i-E_{\mathrm{th}}+h\nu) \tag{1}$$

and

$$\mathrm{He}(1s^2\,^1S)+e^-(E_i)\rightarrow\mathrm{He}(1s2s\ ^3S)+e^-(E_f=E_i-E_{\mathrm{th}}). \tag{2}$$

Measurements of the He $1\,^1S\rightarrow 2\,^3S$ transition for SEPE in the presence of a continuous wave CO_2 laser and those for DEE were first reported by Mason and Newell [1] for incident electron energy close to threshold ($E_{\mathrm{th}}=19.817$ eV) of $2\,^3S$ excitation. The SEPF type of interaction has practical bearing in the heating of plasmas by radiation and laser induced gas break down processes. Study of the process is also of fundamental importance in the understanding of three body interactions. It is of note that along with excitation the interaction changes the polarity of the electron spin. The spin exchange interaction is by definition the interaction that causes the difference between singlet and triplet scattering. Spin exchange due to scattering of electron from atom may occur (1) by exchange of a polarized incident electron with a bound electron of opposite parity and (2) by spin-orbit interaction between the incident electron and the atom. However, spin-orbit interaction causing spin flip is negligible in the case of light atoms because of the small value of the spin-orbit coupling [2]. As such, SEPE and DEE occur in He due to the first mechanism.

The $2\,^3S$ stationary state lies at an energy E_{th} ($=19.817$ eV) above the $1\,^1S$ ground state. No stationary state exists between $1\,^1S$ and $2\,^3S$ states since the $2\,^1S$ metastable state lies 0.797 eV above the $2\,^3S$ state. For the incident electron energy $E_i<E_{\mathrm{th}}$, the SEPE is accomplished by the absorption of one quantum $h\nu$ of radiation combined with electron-atom scattering, in which the electron provides the energy decrement (E_{th}-$h\nu$) required to excite the $2\,^3S$ state. Eventually, the reaction SEPE, where soft photon and electron of energy less than threshold participate simultaneously to excite the atom, must proceed via virtual intermediate states. The following three mechanisms are broadly responsible for excitation of He to triplet state by scattering spin polarized electron in the field of photon: (1) Photon-electron interaction dresses up the electron to a virtual state after which the electron-atom collision will excite the atom accompanied by electron exchange [Fig. 1(a)]. (2) The collision between electron and atom first raises the atom to a virtual state with electron exchange after which the photon is absorbed and excitation occurs [Fig. 1(b)]. (3). The photon dresses up the atom to a virtual state after which electron-atom collision will cause electron exchange and excitation of the atom [Fig. 1(c)]. The SEPE by electron exchange is the sum of these three third order Feynman diagrams. However, the Feynman diagram in which photon is absorbed by scattered electron after electron-atom direct excitation with exchange, will not contribute to the SEPE process.

Direct excitation (DEE) of He in a similar transition with the photon off corresponds to second-order diagram [Fig. 1(d)]. With a soft photon ($h\nu=0.117$ eV) simultaneously with an incident spin polarized electron of energy (E_i) the ratio of the cross sections $\sigma_s(E_i+h\nu)$ for SEPE relative to the cross section $\sigma_D(E_i)$ for DEE is found to lie between $\propto$ and 3×10^{-3} for $E_{\mathrm{th}}<E_i<20$ eV. With the increase of E_i above threshold DEE dominates over SEPE. The result agrees in principle with the experimental results of Mason and Newell [1]. Contribution from the diagram [Fig. 1(b)], where photon absorption by atom occurs after Coulomb interaction, is found to be two order of magnitude higher than that from [Fig. 1(a)] and [Fig. 1(c)].

The other theoretical treatments of the problem to mention are by Raman and Faisal [3] and by Jetzke *et al.* [4], but at high laser power and high incident electron energies. These calculations by their nature neglect the spin exchange, which is present in the current work.

II. THEORETICAL FORMALISM

In QED a composite system of bound particles are represented by a string of field operators operating on particle vacuum and multiplied by unperturbed solution of the Schrö-

*Address correspondence to 370/1, N.S.C. Bose Road, Calcutta 700047, India.

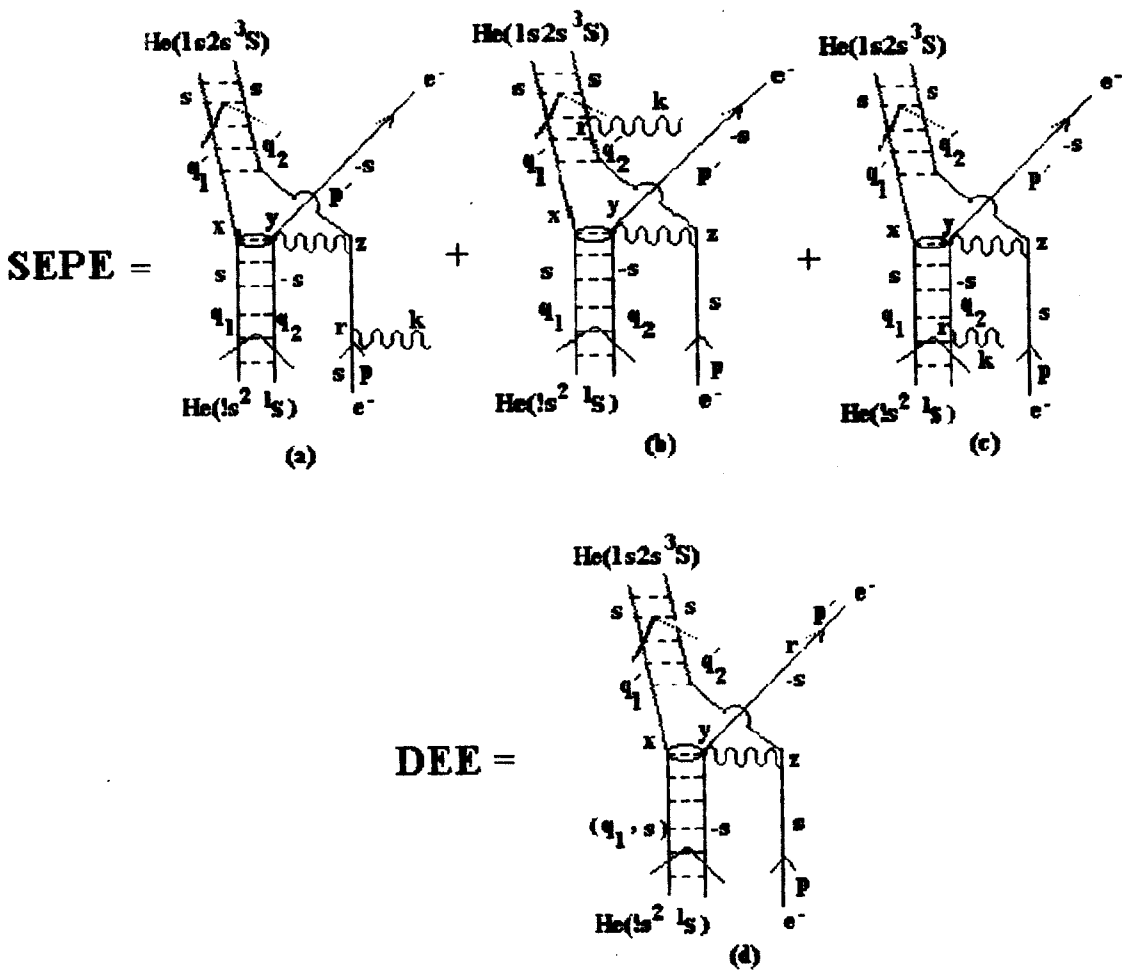

FIG. 1. Feynman diagrams representing the different interactions of the electron and photon. (a), (b), and (c) are for the SEPE process and (d) is for the DEE process. The photon is denoted by a wavy line, the electron by a straight arrowed line, and the atom by a ladder configuration.

dinger equation [5]. Creation and annihilation operators of the particles bound to the Coulomb field of the nucleus obey equal time commutation relations. There will be no loss of generality to represent the bound electrons by the Feynman directed lines. The SEPE reaction under consideration is given by the sum of the amplitudes from the three third order Feynman diagrams. The third order S matrices contain current-current interactions between the incident spin-polarized electron and a bound electron of opposite parity, a photon propagator, and an electron propagator. The three diagrams differ in their position of absorption of the incident photon. In Fig. 1(a) incident electron absorbs the photon and then interacts with the atom. In Figs. 1(b) and 1(c) photon is absorbed by atom after and before electron-atom interaction, respectively. The DEE process is given by the second order Feynman diagram [Fig. 1(d)]. Wave function of the bound electrons in the initial and in the final state are, respectively [6],

$$\Psi_{1\,^1s}^{(s,-s)}(r_1,r_2,R)=\frac{1}{(2\pi)^3}\sqrt{\frac{m^2}{\varepsilon_{q_1}\varepsilon_{q_2}}}\,\Phi_{1\,^1s}(x,y)u(s,q_1)\times u(-s,q_2)e^{i(q_1r_1+q_2p_2+RL)} \tag{3}$$

and

$$\Psi_{2\,^3s}^{(s,s)}(r_1,r_2,R)=\frac{1}{(2\pi)^3}\sqrt{\frac{m^2}{\varepsilon_{q_1}\varepsilon_{q_2}}}\,\Phi_{2\,^3s}(x,y)u(s,q_1')\times u(s,q_2')e^{i(q_1'r_1+q_2'p_2'+RL')}, \tag{4}$$

$\vec{x}=\vec{r}_1-\vec{R}$, $\vec{y}=\vec{r}_2-\vec{R}$ where x,y are the coordinates of the bound electrons relative to the center of mass (c.m.) coordinate R with (c.m.) momentum L.

$\Phi_{1\,^1s}(x,y)$ and $\Phi_{2\,^3s}(x,y)$ are, respectively, the ground singlet state and $1s\,2s$ triplet state of the He atom. $u(s,q)$ is the electron spinor where s and q are, respectively, the spin and momentum of the electron. The ground state and $1s\,2s$ state wave functions of He are, respectively [4],

$$\Phi_{1s^2\,^1S}(x,y)=X_{1s}(x)X_{1s}(y)$$

and

$$\Phi_{1s2s\,^3S}(x,z)=\Gamma[e^{-2x}X_{2s}(z)+e^{-2z}X_{2s}(x)],$$

where $X_{1s}(x)=Ae^{-z_1x}+Be^{-z_2x}$, $A=0.7349$, $B=0.799$, $z_1=1.41$, $z_2=2.61$, $\Gamma=0.6451/[\pi(1+0.06996^2)^{1/2}]$, $X_{2s}(x)=e^{(-1.136x)}-0.2806xe^{(-0.464x)}$.

For the free electron before and after interaction the wave functions are, respectively,

$$\Psi_{e^-}^{(s)}(z,p)=\sqrt{\frac{1}{v(2\pi)^3}}\sqrt{\frac{m}{E_p}}u(s,p)e^{i(zp)} \tag{5}$$

and

$$\Psi_{e^-}^{(-s)}(z,p')=\sqrt{\frac{1}{v(2\pi)^3}}\sqrt{\frac{m}{E_{p'}}}u(-s,p')e^{i(zp')}. \tag{6}$$

p and p' represent the momenta of the spin polarized electrons of spins s and $-s$, respectively. The wave function of the photon

$$A_\nu(r)=\frac{\lambda^\nu}{\sqrt{2\varpi v(2\pi)^3}}(e^{-ikr}+e^{ikr}),\quad \vec{k}\cdot\vec{\lambda}=0. \tag{7}$$

$\omega=|\vec{k}|$, and k and λ are, respectively, the photon momentum and photon polarization vector. The photopropagator is

$$D(y-z)=\int\frac{d^4q}{(2\pi)^4}e^{-iq(y-z)}\frac{-1}{q^2+i\varepsilon}. \tag{8}$$

The fermion propagator is

$$S_F(z-r)=\int\frac{d^4l}{(2\pi)^4}\frac{e^{-il(z-r)}}{t-m+i\varepsilon}. \tag{9}$$

Below we shall show the computation of the Feynman diagrams corresponding to SEPE and DEE processes for excitation of the He $1\,^1S-2\,^3S$ transition.

A. SEPE process

We use the above functions to write the probability amplitudes R_a, R_b, R_c for Figs. 1(a), 1(b), and 1(c) are, respectively,

$$R_a=\frac{1}{4}(e^2/\hbar c)^{3/2}\int d^4x d^4y d^4z d^4r \times[\overline{\Psi}_{2\,^3S}^{(s,s)}(x,z)\gamma_\mu S_F(z-r)\gamma_\nu A_\nu(r,k)\Psi_{e^-}^{(s)}(r,p)] \times D(y-z)[\overline{\Psi}_{e^-}^{(-s)}(y,p')\gamma_\delta\Psi_{1\,^1S}^{(s,-s)}(x,y)], \tag{10}$$

$$R_b=\frac{1}{4}(e^2/\hbar c)^{3/2}\int d^4x d^4y d^4z d^4r \times[\overline{\Psi}_{2\,^3S}^{(s,s)}(x,r')\gamma_\mu S_F(z-r)\gamma_\nu A_\nu(r,k)\Psi_{e^-}^{(s)}(z,p)] \times D(y-z)[\overline{\Psi}_{e^-}^{(-s)}(y,p')\gamma_\delta\Psi_{1\,^1S}^{(s,-s)}(x,y)], \tag{11}$$

and

$$R_c=\frac{1}{4}(e^2/\hbar c)^{3/2}\int d^4x d^4y d^4z d^4r \times[\overline{\Psi}_{2\,^3S}^{(s,s)}(x,z')\gamma_\mu\Psi_{e^-}^{s}(z,p)] \times D(y-z)[\overline{\Psi}_{e^-}^{(-s)}(y,p') \times\gamma_\nu S_F(y-r)\gamma_\delta A_\delta(r,k)\Psi_{1\,^1S}^{(s,-s)}s(x,r')]. \tag{12}$$

z' and r', the coordinates of the bound electrons relative to the c.m. of the atom, are given by $\vec{z}'=\vec{z}-\vec{R}$ and $\vec{r}'=\vec{r}-\vec{R}$.

We substitute from Eqs. (3)–(9) in Eqs. (10), (11), and (12). After integration over the fourth components of the integration variables and also over $d^3\vec{r}$ and $d^3\vec{l}$ we obtain

$$R_a=\vec{C}\Lambda\frac{1}{4}(e^2/\hbar c)^{3/2}\delta(L_0-L_0'+{}_0k_0+p_0+q_{20}-p_0'-q_{20}') \times\delta(q_{10}'-q_{10})\delta^3(L-L'+k+p-p'),\quad I_aL_{a1}L_{a2}L_a, \tag{13}$$

where

$$\vec{C}=\sqrt{\frac{m^6}{\varepsilon_{q_1'}\varepsilon_{q_1}\varepsilon_{q_2'}\varepsilon_{q_2}E_pE_{p'}2\omega}},\quad \Lambda=(2\pi)^6. \tag{14}$$

The product of spinors in Eq. (13) is $L_{a1}L_{a2}L_{a3}$ and I_a is the overlap integral:

$$L_{a1}=[\overline{u}(s,q_1')u(s,q_1)]_x,\quad L_{a2}=[\overline{u}(-s,p')\gamma_\delta u(-s,q_2)]_y,$$

$$L_{a3}=\left[\overline{u}(s,q_2')\gamma_\mu\frac{1}{(l-m+i\varepsilon)}\gamma_\nu\lambda_\nu u(s,p)\right]_{x,s}, \tag{15}$$

with

$$\vec{I}=-(\vec{p}+\vec{k}),\quad l_0=-(p_0+k_0),\quad q_0=q_{20}-p_0'.$$

The overlap integral

$$I_a=\int d^3\vec{x}d^3\vec{y}d^3\vec{z}d^3q\left\{\frac{\exp[-i\vec{y}\cdot\{\vec{p}+\vec{k}-\vec{p}'\}]\exp[i\vec{z}\cdot(\vec{q}+\vec{p}+\vec{k})]\Phi_{2\,^3s}(x,z)\Phi_{1\,^1s}(x,y)}{(q^2+i\varepsilon)}\right\}. \tag{16}$$

The traces of the γ matrices are calculated as below:

$$L_{a2}L_{a2}^{*}=\overline{u}(-s,p')\gamma_{\delta}u(-s,q_2)\overline{u}(-s,q_2)\gamma_{\delta'}u(-s,p')$$
$$=\mathrm{tr}\left[\Delta(p')\gamma_{\delta}\sum(-s)\Delta(q_2)\gamma_{\delta'}\sum(-s)\right], \quad (17)$$

$$L_{a3}^{*}L_{a3}=\overline{u}(s,q_2')\gamma_{\mu}\frac{\not{l}+m+i\varepsilon}{l^2-m^2}\gamma_{\nu}\lambda_{\nu}u(s,p)\overline{u}(s,p)\gamma_{\nu'}\lambda_{\nu'}$$
$$\times\frac{\not{l}+m+i\varepsilon}{l^2-m^2}\gamma_{\mu'}u(s,q_2')$$
$$=\frac{1}{(l^2-m^2)^2}\mathrm{tr}\left[\gamma_{\mu}(\not{l}+m)\gamma_{\nu}\lambda_{\nu}\right.$$
$$\left.\times\sum(s)\Delta(p)\gamma_{\nu'}\lambda_{\nu'}(\not{l}+m)\gamma_{\mu'}\sum(s)\Delta(q_2')\right], \quad (18)$$

where the covariant Dirac projection operators for energy and spin are, respectively, $\Delta(p)=(\not{p}+m)/2m$ and $\Sigma(s)=(1+\gamma_5)/2$ such that $s^{\mu}p_{\mu}=0$ and $L_{a1}L_{a1}^{*}=\delta(q_1-q_1')$.

The overlap integral in R_a [Eq. (13)]

$$I_a=\int I(x,y)e^{-i\vec{y}\cdot\{\vec{p}+\vec{k}-\vec{p}'\}}d^3xd^3y, \quad (19)$$

where

$$I(x,y)=\int e^{i\vec{z}\cdot(\vec{p}+\vec{k})}\frac{e^{i\vec{z}\cdot\vec{q}}}{q_0^2-q^2}\Phi_{1s2s\,{}^3s}(x,z)\Phi_{1s^2\,{}^1s}(x,y)d^3qd^3z.$$

For integration over $d^3\vec{q}$ we use the result

$$\int\frac{e^{-izq}}{q_0^2-q^2+i\varepsilon}d^3q=-\frac{2\pi^2}{z}\cos(zq_0).$$

The amplitude from Fig. 1(b) after some integration can be written as

$$R_b=\vec{C}\Lambda\frac{1}{4}(e^2/\hbar c)^{3/2}$$
$$\times\delta(L_0-L_0'+{}_0k_0+p_0+q_{20}-p_0'-q_{20}')\delta(q_{10}'-q_{10})$$
$$\times\delta^3(L-L'+k+p-p')\int I_bL_{b1}L_{b2}L_{b3}d^3q, \quad (20)$$

where

$$I_b=-\int\frac{\exp i\{-r(\vec{q}+\vec{p}-\vec{k})+y(\vec{q}+\vec{p}')\}\Phi_{1s2s\,{}^3s}(x,r')\Phi_{1s^2\,{}^3s}(x,y)}{(q_0^2-\vec{q}^2)(\vec{p}+\vec{q})^2}d^3r'd^3xd^3y.$$

The expressions for L_{b1}, L_{b2}, and L_{b3} are identical, respectively, to the expressions for L_{a1}, L_{a2}, and L_{a3}. However, in R_b, $l_0=p_0+q_{20}-p_0'$, $\vec{l}=\vec{p}+\vec{q}$, and $q_0=q_{20}-p_0'$,

$$L_{b2}L_{b2}^{*}=\overline{u}(-s,p')\gamma_{\delta}u(-s,q_2)\overline{u}(-s,q_2)\gamma_{\delta'}u(-s,p')=\mathrm{tr}\left[\Delta(p')\gamma_{\delta}\sum(-s)\Delta(q_2)\gamma_{\delta'}\sum(-s)\right],$$

$$L_{b3}^{*}L_{b3}=\overline{u}(s,q_2')\gamma_{\mu}\frac{\not{l}+m+i\varepsilon}{l^2-m^2}\gamma_{\nu}\lambda_{\nu}u(s,p)\overline{u}(s,p)\gamma_{\nu'}\lambda_{\nu'}\frac{\not{l}+m+i\varepsilon}{l^2-m^2}\gamma_{\mu'}u(s,q_2')$$
$$=\frac{l}{(l^2-m^2)^2}\mathrm{tr}\left[\gamma_{\mu}(\not{l}+m)\gamma_{\nu}\lambda_{\nu}\sum(s)\Delta(p)\gamma_{\nu'}\lambda_{\nu'}(\not{l}+m)\gamma_{\mu'}\sum(s)\Delta(q_2')\right],$$

and $L_{b1}L_{b1}^{*}=\delta(q_1-q_1')$.

The amplitude from Fig. 1(c) similarly becomes

$$R_c=\vec{C}\Lambda\frac{1}{4}(e^2/\hbar c)^{3/2}\delta(L_0-L_0'+{}_0k_0+p_0+q_{20}-p_0'-q_{20}')\delta(q_{10}'-q_{10})$$
$$\times\delta^3(L-L'+k+p-p')I_cL_{c1}L_{c2}L_{c3}, \quad (21)$$

with

$$I_c=\int\frac{\exp i\{y(\vec{q}+\vec{p}'-\vec{k})-z(\vec{q}+\vec{p})\}\Phi_{1s2s\,{}^3S}(x,z')\Phi_{1s^2\,{}^3S}(x,r')}{(q_0^2-\vec{q}^2)}d^3r'd^3xd^3yd^3z'd^3q, \quad (22)$$

$$L_{c1}=L_{b1},\quad L_{c2}=[\overline{u}(s,q_2')\gamma_\mu u(s,p)]_z,$$

$$L_{c3}=\left[\overline{u}(-s,p')\gamma_\mu\frac{1}{(\not{l}-m+i\varepsilon)}\gamma_\delta\lambda_\delta u([-s,q_2)\right]_{y,r},$$

$$l=-k,\quad q_0=q_{20}-p_0'+k_0.$$

Spin $s(0,\vec{s}/|s|)$ and photon polarization vector $\lambda(0,\vec{\lambda}/|\lambda|)$ are such that $s^2=\lambda^2=-1$. Further $\vec{k}\cdot\vec{\lambda}=0$ and $\vec{p}\cdot\vec{s}=0$ and for simplicity of calculation we assume photon momentum $\vec{k}$ to be perpendicular to $\vec{s}$ and $\vec{p}$. The traces in Eqs. (17) and (18) then become

$$\begin{aligned}L_{a3}L_{a3}^*=&-\{64m^4+m^3[32(-E+\varepsilon_{2s}+k_0)]\\&+m^2[16E\varepsilon_{2s}+32k_0\varepsilon_{2s}-32k_0^2]\\&+m[-32k_0^2(E-\varepsilon_{2s})+64Ek_0\varepsilon_{2s}]\\&+[32k_0^2E\varepsilon_{2s}+64E^2k_0\varepsilon_{2s}]\}/16m^2(l^2-m^2)^2,\end{aligned}\tag{23}$$

$$L_{a2}L_{a2}^*=[4m^2-8m(E'-\varepsilon_{1s})+8\varepsilon_{1s}E']/16m^2.\tag{24}$$

Traces for other diagrams are calculated similarly.

B. DEE process

The amplitude for direct electron excitation $R_{\rm DEE}$ of He in transition $1\,^1S\rightarrow 2\,^3S$ by spin polarized electron [Fig. 1(d)] is given by

$$\begin{aligned}R_{\rm DEE}=&\vec{\vec{C}}\Lambda\frac{1}{4}(e^2/\hbar c)\\&\times\delta(p_0+q_{20}-p_0'-q_{20}')J_{\rm DEE}T_1T_2d^3xd^3yd^3zd^3q,\end{aligned}\tag{25}$$

where

$$J_{\rm DEE}=\int J(x,y,z)\frac{\exp[i\vec{q}(\vec{y}-\vec{z})]}{|\vec{q}_0^2-\vec{q}^2|}d^3qd^3xd^3yd^3z,$$

$$J(x,y,z)=\Phi_{1s2s\,^3S}(x,z)\Phi_{1s^2\,^3S}(x,y)\exp[i(\vec{p}\cdot\vec{z}-\vec{p}\cdot\vec{y})],$$

$$T_1=[\overline{u}(-s,p')\gamma_\delta\overline{u}(-s,p')]_y,$$

$$T_2=[\overline{u}(s,q_2')\gamma_\mu\overline{u}(s,p)]_z.$$

The traces are calculated as before.

III. RESULTS AND DISCUSSIONS

Cross sections SEPE and DEE for transition $1\,^1S\rightarrow 2\,^3S$ in He by spin polarized electrons are given, respectively, by

$$\sigma_s=\int\frac{m}{|\vec{p}+\vec{k}|}|R_a+R_b+R_e|^2\frac{d^3p'}{(2\pi)^3},\tag{26}$$

$$\sigma_d=\int\frac{m}{|\vec{p}|}|R_{\rm dee}|^2\frac{d^3p'}{(2\pi)^3}.\tag{27}$$

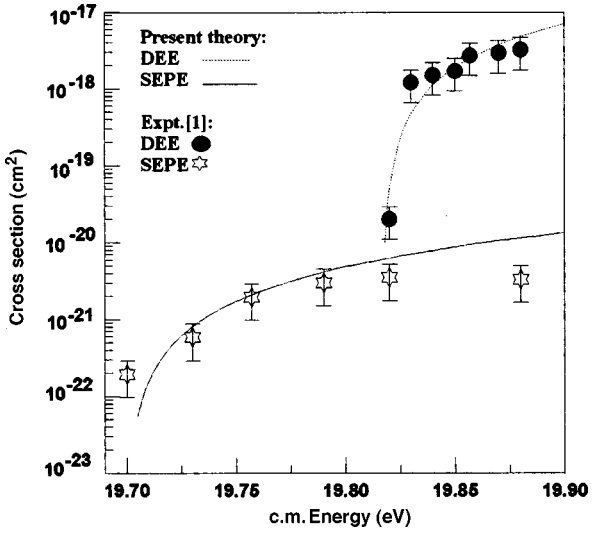

FIG. 2. Simultaneous electron-photon excitation (SEPE) and direct electron excitation (DEE) of He in the transition $1\,^1S$ to $2\,^3S$ versus incident electron energy (c.m.). The energy of the photon is 0.117 eV. Experimental data is from Mason and Newell [1], the energy of the photon being 0.117 eV derived from a cw CO_2 laser beam (300 W).

To include the effect of Coulomb distortion the cross sections are multiplied by the square of the Sommerfeld factor $F(\eta)$, where

$$F(\eta)=\Gamma(1+i\eta)\exp(-\pi\eta/2),\quad \eta=2\pi m/|p|.\tag{28}$$

The integrations are done by using Gaussian quadrature. The maximum contribution in SEPE is found to come from Fig. 1(b) where photon absorption occurs after electron exchange interaction between the incident spin polarized electron and a bound electron of opposite parity. Contributions from Figs. 1(a) and 1(c) are 2 orders of magnitude smaller than those from Fig. 1(b). The interference terms are also very small compared to the $|R_b|^2$. Hence the dominant SEPE diagram [Fig. 1(b)] is the one where photon absorption by the atom occurs after electron-bound electron exchange interaction.

We have calculated the direct electron excitation (DEE) cross section to the triplet $2\,^3S$ state due to interaction between a spin polarized incident electron and a bound electron of opposite parity. The DEE interaction corresponds to a second order diagram [Fig. 1(d)]. The energy range covered (9.817 to 20 eV) is below $2\,^1S$ metastable state (20.614 eV). There is a rapid rise in the cross section in that range which compares well with the result of Mason and Newell (Fig. 2). The ratio $\sigma_s(E_i+h\nu)/\sigma_d(E_i)$ plotted (Fig. 3) for the energy range $19.847<E_i\leqslant 20$ eV is found to fall rapidly from infinity to 3×10^{-3}. As the incident electron energy increases above threshold of excitation, DEE cross section dominates the metastable excitation process.

The SEPE is a third order process corresponding to the third order S matrix whereas DEE is a given by the second order S matrix. With $E_i>E_{\rm th}$ the ratio of the SEPE cross section to the DEE cross section is of the order 3.7×10^{-3} at $E_i=19.9$ eV, corresponding experimental value being 1.4×10^{-3}. The experimental absolute value of the cross section for SEPE (photon energy 0.117 eV) is obtained by normal-

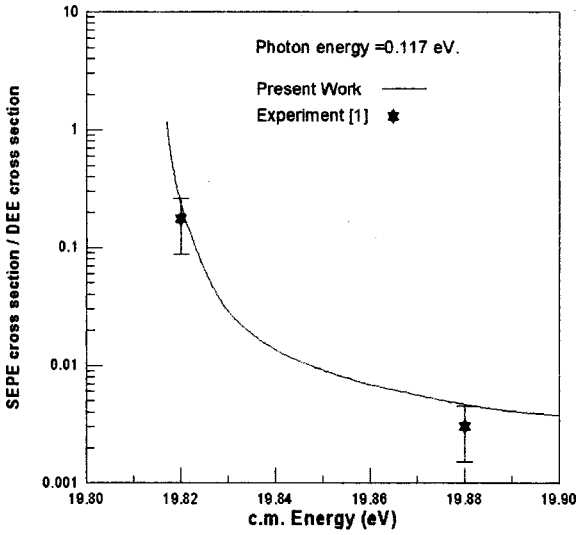

FIG. 3. Ratio of the cross sections for SEPE to DEE. The continuous curve is from the present calculation. Experimental data as in Fig. 2.

izing the experimental value [1] given in arbitrary unit by the corresponding theoretical value at $E_i = 19.757$ eV.

IV. CONCLUSION

The experimental study of SEPE has raised many questions regarding the ordering of photon absorption in the exchange excitation process. Does the electron absorb a photon prior to colliding with the atom or does the atom go to some virtual dressed state by photon absorption prior to electron collision or does the electron scattering occurs prior to photon absorption by the atom? Through the present study we have tried to answer these questions. The three questions raised correspond to Figs. 1(a), 1(c), and 1(b), respectively. A diagram corresponding to absorption of photon by the scattered electron after collisional excitation of the atom with exchange, where photon-electron interaction changes only the dynamics of the scattered electron, does not belong to the SEPE process. Calculation of the Feynman diagrams corresponding to the SEPE process provides an idea regarding the ordering of the photon absorption. The experimental values of the SEPE and DEE [1] are plotted in Fig. 2 along with the theoretical results. Although in the experiment the incident electrons are unpolarized, physically one may assume of all the incident electrons those with necessary spins to participate in the exchange interaction. This justifies the comparative study of the present work with the experimental results. From the general trend of the present curve we find that the theoretical prediction compares well with experimental results. Experiments on scattering of spin polarized electron from two-electron atomic and ionic targets are necessary to verify the present formalism.

ACKNOWLEDGMENTS

S.B. expresses thanks to Professor F. H. M. Faisal of Bielefeld, Germany, for the encouragement to calculate the above problem in a field theoretic way. The work was supported by UGC, New Delhi, under Major Research Project No. F10-17/98(SR-I).

[1] N. J. Mason and W. R. Newell, J. Phys. B **22**, 777 (1989).
[2] J. Kessler, in *Atomic Physics 12*, edited by Jens C. Zorn and Robert R. Lewis, AIP Conf. Proc. No. 233 (AIP, New York, 1991).
[3] N. K. Raman and F. H. M. Faisal, J. Phys. B **9**, L275 (1976).
[4] S. Jetzke, F. H. M Faisal, R. Hippler, and H. O. Lutz, Z. Phys. A **315**, 271 (1984).
[5] S. Bhattacharyya, K. Rinn, E. Salzborn, and L. Chatterjee, J. Phys. B **21**, 111 (1988).
[6] S. Bhattacharyya and K. Pathak, Phys. Scr. **54**, 143 (1996).